Pezo, M. L., *et al.*: Numerical Prediction of Nucleate Pool Boiling Heat Transfer …
THERMAL SCIENCE, Year 2016, Vol. 20, Suppl. 1, pp. S113-S123

S113

NUMERICAL PREDICTION OF NUCLEATE POOL BOILING HEAT TRANSFER COEFFICIENT UNDER HIGH HEAT FLUXES

by

Milada L. PEZO[a*] and Vladimir D. STEVANOVIĆ[b]

[a] Laboratory for Thermal Engineering and Energy, Vinca Institute of Nuclear Sciences,
University of Belgrade, Belgrade, Serbia
[b] Faculty of Mechanical Engineering, University of Belgrade, Belgrade, Serbia

This paper presents computational fluid dynamics approach to prediction of the heat transfer coefficient for nucleate pool boiling under high heat fluxes. The 3-D numerical simulations of the atmospheric saturated pool boiling are performed. Mathematical modelling of pool boiling requires a treatment of vapor-liquid two-phase mixture on the macro level, as well as on the micro level, such as bubble growth and departure from the heating surface. Two-phase flow is modelled by the two-fluid model, which consists of the mass, momentum, and energy conservation equations for each phase. Interface transfer processes are calculated by the closure laws. Micro level phenomena on the heating surface are modelled with the bubble nucleation site density, the bubble resistance time on the heating wall and with the certain level of randomness in the location of bubble nucleation sites. The developed model was used to determine the heat transfer coefficient and results of numerical simulations are compared with available experimental results and several empirical correlations. A considerable scattering of the predictions of the pool boiling heat transfer coefficient by experimental correlations is observed, while the numerically predicted values are within the range of results calculated by well-known Kutateladze, Mostinski, Kruzhilin, and Rohsenow correlations. The presented numerical modelling approach is original regarding both the application of the two-fluid two-phase model for the determination of heat transfer coefficient in pool boiling and the defined boundary conditions at the heated wall surface.

Key words: *pool boiling, heat transfer coefficient, computational fluid dynamics*

Introduction

Boiling of liquids has been a research topic for a long time. Two and a half centuries ago a droplet evaporation on the hot surface was observed by Leidenfrost [1] and this phenomenon is related to the film boiling. Other modes of boiling phenomenon were experimentally observed and presented by Nukiyama [2] through his well-known boiling curve. Boiling crisis and critical heat flux values were investigated more than half a century ago by Kutateladze [3, 4] and Zuber [5]. The modes of boiling are still a topic of extensive research due to their importance for the design of safe, reliable and efficient operation of various thermal equipment and because of the complexity of their physical phenomena.

Thermal equipment with vapour generation is designed to operate under nucleate boiling conditions. Nucleate boiling provides orders of magnitude higher heat transfer coeffi-

---
* Corresponding author; e-mail: milada@vinca.rs

S114

Pezo, M. L., *et al.*: Numerical Prediction of Nucleate Pool Boiling Heat Transfer …
THERMAL SCIENCE, Year 2016, Vol. 20, Suppl. 1, pp. S113-S123

cients than one phase convective heat transfer. A number of experimental and semi-experimental correlations for the determination of nucleate boiling heat transfer coefficient have been developed in the past. Some well-known correlations that are used in engineering practice are mentioned, such as the correlations developed by Kutateladze and Borishanski [6], Kutateladze [7], Kruzhilin [8], Mostinski [9], and Rohsenow [10]. These correlations are suitable for a wide range of fluids and heating surfaces, but their predictions of heat flux might considerably differ from each other. More reliable predictions can be achieved by correlations that take into account the heated wall-fluid combination, as presented by Pioro *et al.* [11]. For instance, the Rohsenow correlation [10] comprises two parameters that depend on the heated wall and fluid combination, one parameter multiplies the terms in the correlation and the other is the power of the Prandtl number. A disadvantage of the experimentally based correlations is the uncertainty of their predictions in cases when thermal hydraulic parameters of the analyzed problem do not match the experimental ranges that were the basis for the correlations development.

The governing mechanisms of the nucleate boiling were presented among others by Dhir [12]. These are the number density of nucleation sites, the bubble diameter at departure, the bubble release frequency. In addition, the experimental work of Theofanous *et al.* [13, 14] showed that there is a strong influence of the heaters surface on the boiling process. Their experimental investigation showed that the boiling characteristics are influenced not only by the hydrodynamic conditions in the vicinity of the heated surface, but also by the heater's surface micro-conditions, which they characterized as fresh, medium aged, and heavily aged surfaces. They determined the nucleation site density for each age type of heater's surface. Surface roughness, boiling liquid wetting ability and present impurities have strong influence on complex processes on the micro-scale level at the heated surface. The energy balances of bubble growth were reviewed by Kim [15]. The heat transfer from the heated wall to the boiling two-phase mixture was divided into convection from the heated wall to the liquid, conduction through the micro-layer between the wall and the bottom of the growing bubble and from the surrounding superheated liquid layer to the evaporating bubble interface cap. These micro conditions between the heated wall and the growing bubbles were incorporated into the model for the numerical simulation of one or several bubbles growth onto the heated wall by Dhir [12] and Son and Dhir [16]. Isolated bubbles formation under lower values of heat flux up to 4-5 W/cm^2 was presented for water boiling in [12]. Under high heat fluxes the bubbles merging and the formation of larger steam volumes on the heated wall were presented in [16]. In the simulations presented in [12, 16] the wall transient heat conduction due to heating and cooling by the boiling liquid was not considered. Instead, the constant temperature is prescribed for the wall surface in contact with the boiling fluid. Numerical simulation of the fluid F72 boiling with the growth of hundred bubbles is presented in [17]. The simulation of the growth of a large number of bubbles on the heated wall was achieved by the hybrid model that completely solves the 3-D time-dependent energy equation in the heated wall, but applies a semi-empirical simplified models of the phenomena occurring on the boiling liquid side. A simulation of the single bubble growth with the solving of the heated wall transient conduction was reported in [18].

The aim of this paper is to present a 3-D modelling approach that enables numerical prediction of the nucleate boiling heat transfer coefficient by taking into account both the heated wall characteristics and the two-phase mixture dynamics on the heated wall. The characteristics of the wall surface in contact and interaction with the boiling fluid are expressed through the nucleation site density, the liquid wetting angle and the bubble residence time on the heated wall. The two-phase mixture dynamics is modelled by the two-fluid model and cor-

responding correlations for the mass, momentum, and energy transfer at the liquid and vapour interface surfaces. Numerically predicted heat transfer coefficients are compared with predictions of several engineering correlations and experimental results of Theofanous *et al.* [13, 14], and the level of agreement is shown for nucleate boiling under high heat fluxes close to the critical heat flux values. The simulated boiling conditions under high heat fluxes are important for the design of efficient and economic heat transfer surfaces. At the same time the high heat fluxes are close to the critical heat flux values, which might endanger the thermal safety and lead to the burn-out of heated walls.

Description of the pool boiling model

In the present work the pool boiling process is investigated by the application of the two-fluid model for the prediction of water-vapor two-phase mixture conditions on the heated horizontal wall. The generated steam upward flow from the heated wall surface and the water circulation in the pool are predicted by solving the mass, momentum, and energy balance equations for each (vapour and liquid) phase. The interface transfer processes between the liquid and vapor phase, *i. e.* the interface friction and the evaporation rate are calculated by appropriate closure laws. The two-fluid model is coupled with the model of transient 3-D heat conduction in the heated wall. The boundary conditions between the heated wall and the boiling two-phase mixture above it are modelled with the bubble nucleation site density, the bubble residence time on the heated wall and with a certain level of randomness to the location of bubble nucleation sites. Here presented modelling approach was previously applied for the prediction of the critical heat flux values [19].

Pool boiling is simulated in the square vessel, initially filled with the saturated water up to 0.02 m, fig. 1. The vessel is at atmospheric pressure. The bottom wall is made of copper, with a high conductivity and heated by the uniform volumetric heating source. The heat conductivity through the wall is simulated.
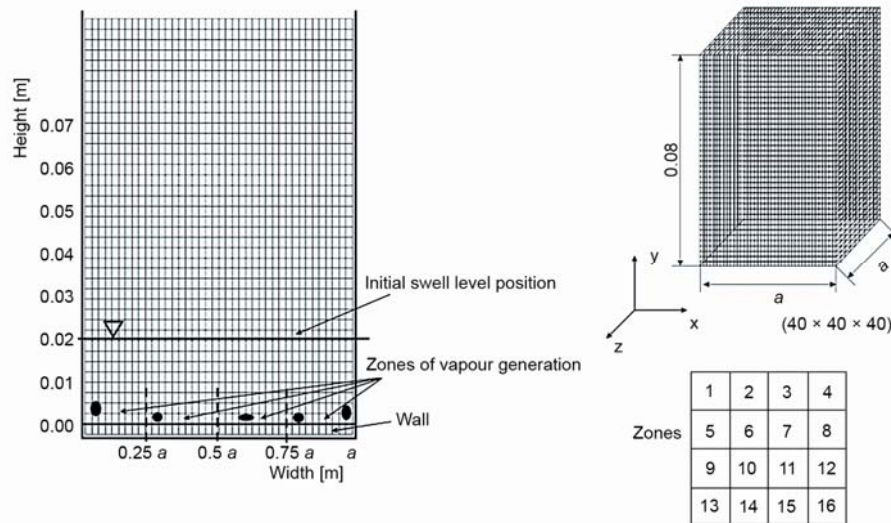

Figure 1. Numerical grid used in the simulation of pool boiling

S116

Pezo, M. L., *et al.*: Numerical Prediction of Nucleate Pool Boiling Heat Transfer …
THERMAL SCIENCE, Year 2016, Vol. 20, Suppl. 1, pp. S113-S123

The heat transfer from the heater's surface towards the liquid or vapor phase in control volumes without vapor generation is neglected, *i. e.* the sensible heat transferred to the liquid or vapor phase is neglected. Hence, the heat transfer from the heater's surface towards the fluid takes place at the nucleation sites and it is totally consumed in the vapor generation. This assumption is valid for nucleate boiling under high heat flux conditions due to the high nucleation site density and high heat loads transferred from the heated wall towards the growing bubbles. In addition, this assumption is supported by the numerical analyses in the chapter *Micro-scale parameters* based on the micro-level characteristics of bubble growth on the heated wall. In the chapter *Micro-scale parameters* it is shown that the averaged heat transfer coefficient based on the heat transfer to the growing bubbles is orders of magnitude higher than the heat transfer coefficient due to the convection from the heated wall to the liquid phase.

Vapor bubbles are generated at the bottom wall (fig. 1). During the vapor generation, the swell level location dynamically changes. The prediction of the swell level position is also included in this model. The volume above the swell level is filled with vapor.

The bottom wall is divided into zones, fig. 1, and each zone corresponds to one nucleation site. The width of the square zone is varied according to the nucleation site density. In general, it depends on the wall roughness and wall superheating [12]. Each zone comprises ten or more control volumes. The grid refinement tests have shown that with ten or more control volumes within a nucleation zone there is no change in the calculated critical heat flux or two-phase flow structure in the pool boiling. A location of bubble generation is randomly chosen among the control volumes comprised within a zone, where during the time only one bubble is generated within each zone. As noted, it is assumed that the major portion of the heat is transferred at the nucleation site, and convective heat transfer from the wall to the one-phase fluid is neglected. The relation between the density of nucleation sites n and the zone width b can be derived from the simple geometric condition that one square meter is covered with n nucleation sites, *i. e.*:

$$b = \frac{1}{\sqrt{n}} \tag{1}$$

Therefore, the zone width is 0.01 m × 0.01 m for the nucleation site density 1 cm^{-2}, 0.003 m × 0.003 m for the density 11 cm^{-2}, 0.002 m × 0.002 m for 25 cm^{-2}, 0.0016 m × 0.0016 m for 39 cm^{-2}, and 0.0014 m × 0.0014 m for the nucleation site density 51 cm^{-2}. These nucleation site densities are in the range of experimentally determined values by Theofanous *et al.* [13, 14] for fresh and aged heaters made of titanium films and copper walls. The same range of nucleation site densities was measured by Qi *et al.* [20] in experiments of water depressurisation and dissolved air bubbles nucleation on the stainless steel surface, while in experiments with the brass surface even higher nucleation site densities up to 250 cm^{-2} were observed for the highest depressurisations.

The period of vapor generation at a randomly chosen location (nucleation site) is equal to the bubble residence time on the heater's surface, as determined in the following chapter.

Micro-scale parameters

The applied micro-scale model of bubble grow on the heater surface was already presented in [19]. The water capillarity length is used for scaling the infinite geometry, and is given by:

Pezo, M. L., *et al.*: Numerical Prediction of Nucleate Pool Boiling Heat Transfer …
THERMAL SCIENCE, Year 2016, Vol. 20, Suppl. 1, pp. S113-S123

S117

$$L_c = \sqrt{\frac{\sigma}{g(\rho_1 - \rho_2)}} \tag{2}$$

and for water at atmospheric conditions, it is equal to $2.5 \cdot 10^{-3}$ m. Even in case of high nucleation site density of 51 cm^{-2} the heater width is 22 times longer than the characteristic capillary length.

The nucleation site density is determined with the heat flux, heating surface roughness, wetting contact angle and thermo-physical characteristics of the boiling fluid and the wall. In the present modelling research, the values of the nucleation site densities are prescribed input values and they represent the complexity of all conditions stated in the foregoing sentence.

The second parameter that determines the pool boiling dynamics is the bubble residence time on the heater surface. This is the time of bubble growth up to the bubble departure diameter. It is determined by starting from the expression for the bubble diameter at departure from the heated wall [21]:

$$D_b = 0.0208 \, \theta \, L_c \tag{3}$$

and from the relation between the bubble diameter and the bubble growth time [22]:

$$D_b = 2\left(\gamma \mathrm{Ja} + \sqrt{\gamma^2 \mathrm{Ja}^2 + 2\beta \mathrm{Ja}}\right)\sqrt{a\tau} \tag{4}$$

where Ja is the Jacob number:

$$\mathrm{Ja} = \frac{c_{p1}\Delta T_w}{h_{12}}\frac{\rho_1}{\rho_2} \tag{5}$$

In [22] it is reported that for contact angles between 40° and 90° the parameter γ is 0.1 to 0.49, respectively. The empirical parameter β is equal to 6. Equation (4) is applicable to the general case when the heat is transferred to the growing bubble both from the heating surface into the root of a bubble and from the superheated liquid layer around the bubble.

By substituting eq. (3), which determines the separation bubble diameter, into eq. (4) the bubble residence time on the heating surface is derived in the form:

$$\tau = \frac{(0.0208\theta)^2 L_c^2}{4a_1\left(\gamma \mathrm{Ja} + \sqrt{\gamma^2 \mathrm{Ja}^2 + 2\beta \mathrm{Ja}}\right)^2} \tag{6}$$

as the function of wetting contact angle θ and the Jacob number. The wall superheating in eq. (5) for the Jacob number is the result of the numerical simulation by the presented model. In this way the bubble residence time in eq. (6) is directly dependent on the heat flux, through the Jacob number, and the contact angle.

The heat transfer coefficient is estimated by eqs. (2)-(6) for the water nucleate boiling at the atmospheric pressure and the corresponding saturation temperature of 100 °C. The water wetting angle of 70°. is assumed and the required parameters for the calculation are: c_p = 4220 J/kgK, a = 16.9·10^{-8} m^2/s, ρ_1 = 958.4 kg/m^3, ρ_2 = 0.598 kg/m^3, σ = 588.6 N/m, h_{12} = 2257 kJ/kg, and γ = 0.334. The assumed wall superheat is ΔT = 20 °C. The bubble diameter at departure is calculated by eq. (3) as 3.64 mm. The Jacob number is 59.9 (eq. 5). Hence, the bubble residence time is calculated by eq. (6) as 6.9·10^{-3} s. The averaged heat transfer rate to the departing bubble is calculated as $\dot{Q}_B = \rho_2 h_{12}\pi D^3/6\tau = 4.9$ W. For the estimated nu-

cleation site density of n = 150,000 sites per m^2 the average heat flux due to the bubble growth is $\dot{q}_A$ = 735,000 W/m^2. Hence, for the assumed heater wall surface superheat of 20 °C, the calculated heat flux is 735,000 W/m^2. This relation is in good agreement with the measured $\Delta T \sim \dot{q}_A$ relation as presented in [13]. Further, this analysis shows that the heater surface cooling by boiling under high heat flux loads is achieved by the bubble growth on the heater surface, *i. e.* the convective heat transfer from the heater to the liquid phase might be neglected. If the same analysis is applied to the lower wall superheat of 10 °C and the nuclea-tion site density of about 30,000 sites per m^2 according to measured values presented in [13], the Jacob number is 30.0 (eq. 5), the bubble residence time is 0.02 s (eq. 6). The other param-eters are the same as in the previous example of the high wall superheat and the calculated heat flux equals 51,098 W/m^2. The measured value of heat flux reported in [13] is in the range of 100,000 W/m^2, which means that about half of the heat is transferred to the growing bubble at the wall, while the second half is transferred by convection from the heaters wall surface to the superheated liquid.

In conclusion, the boundary conditions for the bubble generation are determined by the density of nucleation sites, as a spatial parameter, which is introduced through the width of the zones presented in fig.1, and with the bubble residence time on the heater's wall, as a temporal parameter.

Governing equations

Two different regions are modelled: the boiling two-phase flow in the pool and the transient heat conduction in the heated wall. The 3-D liquid and vapor two-phase flow is modelled by the two-fluid model. The conservation equations for mass, momentum, and en-ergy fluid flow are written for both phases and interface transfer processes are modelled by closure laws.

Mass conservation equation:

$$\frac{\partial \alpha_k \rho_k}{\partial t} + \frac{\partial(\alpha_k \rho_k u_{k,i})}{\partial x_i} = (-1)^k (\Gamma_e - \Gamma_c) \tag{7}$$

Momentum conservation equation:

$$\frac{\partial(\alpha_k \rho_k u_{k,i})}{\partial t} + \frac{\partial(\alpha_k \rho_k u_{k,i} u_{k,j})}{\partial x_j} = -\alpha_k \frac{\partial p}{\partial x_i} +$$
$$+ \alpha_k \rho_k g_i + (-1)^k (\Gamma_e - \Gamma_c) u_{ik,i} + (-1)^{k+1} F_{21,i} \tag{8}$$

Energy conservation equation:

$$\frac{\partial(\alpha_k \rho_k T_k)}{\partial t} + \frac{\partial(\alpha_k \rho_k u_{k,i} T_k)}{\partial x_i} = \frac{\partial}{\partial x_i}\left(k_k \frac{\partial T_k}{\partial x_i}\right) + (-1)^k (\Gamma_e - \Gamma_c) T_k + (2 - k)\frac{\dot{q}_b}{c_{p,k}} \tag{9}$$

where k = 1 for liquid and k = 2 for vapor.

Energy equation for the heated wall:

$$\frac{\partial T}{\partial t} = a\nabla^2 T + \frac{\dot{q}_h}{(\rho c_p)_p} - \frac{\dot{q}_b}{(\rho c_p)_p} \tag{10}$$

where q_h is the volumetric heat source in the wall (for instance the electric heating), while q_b is the heat sink in the control volumes on the wall surface due to the bubble growth, and the heat source in the fluid control volumes on the wall when the bubble growth occurs, fig. 1. It is assumed that the bubble nucleation does not occur, *i. e.* the heat source q_b equals zero, if the void fraction in the control volume on the wall surface is higher than $1\text{-}10^{-5}$.

Closure laws

In order to solve the set of equations it is necessary to use additional correlations for interfacial drag force and intensity of evaporation and condensation rate.

The interfacial drag force:

$$F_{21,i} = \frac{3}{4}\,\alpha_2\rho_1\,\frac{C_D}{D_p}\,\sqrt{\sum_{j=1}^{3}\left(u_{2,j}-u_{1,j}\right)^2}\left(u_{2,i}-u_{1,i}\right) \tag{11}$$

where C_D is interfacial drag coefficient, and D_P is the diameter of the dispersed particle. The interfacial drag coefficient is given in the following term [19]:

$$C_D = 1.487 D_p \sqrt{\frac{g\Delta\rho}{\sigma}}\left(1-\alpha_2\right)^3\left(1-0.75\alpha_2\right)^2 \tag{12}$$

The intensity of evaporation and condensation is calculated with the empirical model that takes into account the phase change relaxation time τ [19]. The intensity of evaporation rate:

$$\Gamma_e = \frac{\alpha_1\rho_1}{\tau_e}\,\frac{h_1-h'}{h''-h'} \tag{13}$$

The intensity of condensation rate:

$$\Gamma_c = \frac{\alpha_1\rho_1}{\tau_c}\,\frac{h'-h_1}{h''-h'} \tag{14}$$

Numerical method

The set of balance equation is solved by using the control volume based finite difference method. Numerical semi implicit method for pressure-linked equations (SIMPLE) is used for solving pressure-correction equation from the momentum and mass balance equations [23]. The 3-D flow field is discretized in Cartesian co-ordinates. Numerical grid is made from $40 \times 50 \times 40$ control volumes. Numerical grid consists of two parts: the heated wall ($40 \times 10 \times 40$ control volumes) and the two phase mixture ($40 \times 40 \times 40$ control volumes), fig. 1.

A discretization of partial differential equations is carried out by their integration over control volumes of basic and staggered grids. The convection terms are approximated with upwind finite differences, while diffusion and source terms are approximated with central differences. Fully implicit time integration is applied. The set of algebraic equations is solved iteratively with the line-by-line three-diagonal-matrix algorithm [23].

The calculation error for every balance equation and every control volume is kept within limits of 10^{-5} by iterative solution of sets of linear algebraic equations.

**Comparison of nucleate boiling heat transfer
coefficients predicted with the numerical simulations,
empirical correlations and from measured data**

The heat transfer coefficients are calculated for the performed numerical simulations of the nucleate boiling based on the prescribed heat load $\dot{Q}$ and the heater area A and the wall superheat $T_w - T_1$:

$$h = \frac{\dot{Q}}{A\left(T_w - T_1\right)} \tag{15}$$

where T_w is the mean temperature of the heater wall surface in contact with the two-phase mixture. These results are compared with the heat transfer coefficients calculated from the measured data presented in [13] and with several well-known empirical correlations.

Mostinski [9] proposed correlation for nucleate pool boiling heat transfer coefficient without taking into consideration the characteristics of the heating surface:

$$h = 0.106 p_c^{0.69} q^{0.7} f(p_R)$$
$$f(p_R) = 1.8 p_R^{0.17} + 4 p_R^{1.2} + 10 p_R^{10} \tag{16}$$

where p_R [bar], is the reduced value of pressure $p_R = p/p_c$ and p_c [bar] is the critical value of pressure.

More complex correlation is proposed by Rohsenow [10]:

$$\frac{c_p \Delta T_b}{h_{fg}} = C_{sf} \left[\frac{q}{\mu h_{fg}} \sqrt{\frac{\sigma}{g(\rho - \rho_g)}} \right]^{0.33} \left(\frac{c_p \mu}{k} \right)^n \tag{17}$$

and $h = q/\Delta T_b$, where $C_{sf} = 0.015$ has constant value and depends on characteristics of heaters surface. Values of C_{sf} and n for various surfaces-fluid combinations of Rohsenow are listed in [10].

Frequently used correlation for nucleate boiling heat transfer coefficient has been Kutateladze and Borishaskii [6] and Kutateladze [7] correlation.

New Kutateladze correlation [8]:

$$\mathrm{Nu} = 3.37 \cdot 10^{-9} K^{-2} M^{-4}$$

where

$$\mathrm{Nu} = \frac{h_b l}{k}, \quad K = \frac{h_{fg} h_b}{c_p q}, \quad M^4 = \frac{\dfrac{\sigma g}{\rho - \rho_g}}{\left(\dfrac{p}{\rho_g}\right)^2}, \quad \text{and} \quad h = \left[3.37 \cdot 10^{-9} \frac{k}{l} \left(\frac{h_{fg}}{c_p q} \right)^{-2} M^{-4} \right]^{\frac{1}{3}} \tag{18}$$

Old Kutateladze correlation [8]:

$$\mathrm{Nu} = 0.44\ K^{0.7}\ \mathrm{Pr}^{0.35} \quad \text{and} \quad \frac{h\,l}{k} = 0.44 \left(\frac{1 \cdot 10^{-4} qp}{g h_{fg} \rho_g \mu} \frac{\rho}{\rho - \rho_g} \right)^{0.7} \mathrm{Pr}^{0.35} \tag{19}$$

Kruzhilin correlation [8]:

$$\frac{h\,l}{k} = 0.082 \left(\frac{h_{fg}q}{g(T_s + 273.15)k} \frac{\rho_g}{\rho - \rho_g} \right)^{0.7} \left(\frac{(T_s + 273.15)c_p\sigma\rho}{h_{fg}^2\rho_g^2 l} \right)^{0.33} \mathrm{Pr}^{-0.45} \qquad (20)$$

Numerical simulations are performed for different heat flux values and for different nucleation cites densities, which should represent different surface roughness's. The results of the numerical simulations, values based on the measured data and results of empirical correlations are shown in fig. 2. A significant scattering of the results is shown. A scattering of measured data is due to the aging of heaters' material [13]. Generally, fresh heaters lead to lower heat transfer coefficient than aged heaters for the same heater wall superheat. The heaters' aging is taken into account in the numerical simulations by the nucleation site densities, which also results in the data scattering. Each applied empirical correlation shows a consistent dependence between heat transfer coefficient and the heater superheat, but the predictions of the correlations are different from one another. Nevertheless, the predictions of the empirical correlations are in the same range as the measured data and the numerical predictions. The Mostinski [9] and the old Kutateladze [6] correlations provide nearly the same predictions that correspond to the boiling conditions on the fresh heaters and corresponding lower nucleation site density values that are applied in the numerical simulations. Kruzhilin [8] and new Kutateladze correlations give values that are in the range of values measured for the aged heaters and numerically predicted with the greater number of nucleation site densities. The average of the values presented in fig. 2 is covered by the Rohsenow [10] correlation. In addition, it should be noted that the experimental values show a steeper $\Delta T \sim h$ dependence, especially in case of fresh heaters and the highest heat flux conditions.

Based on performed numerical simulations and experimental results it can be concluded that surface roughness significantly affects the value of nucleate boiling heat transfer
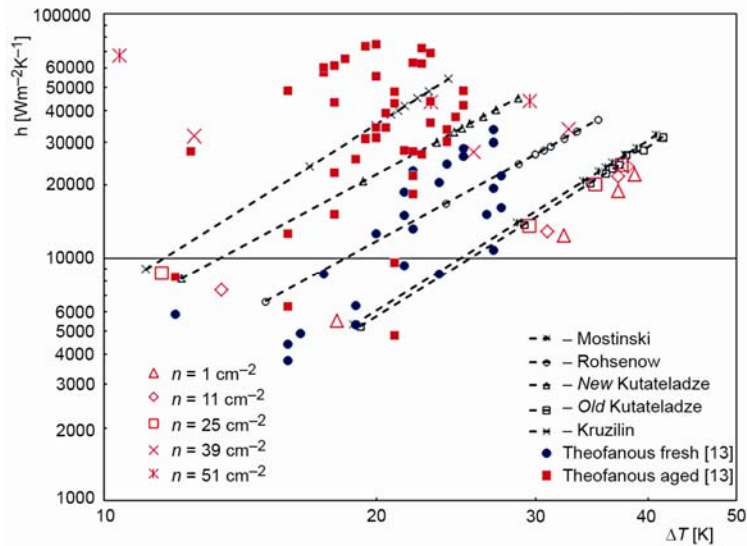

Figure 2. Comparison of the results for nucleate boiling heat transfer coefficient of numerical simulation with experimental results of Theofanous *et al.* [13] and experimental correlations [6-10]

coefficient. A further improvement of the experimental correlations is needed regarding the influence of the heaters surface aging (roughness) on the nucleate boiling.

Conclusions

The 3-D numerical investigation of the nucleate pool boiling under high heat fluxes, close to the critical heat flux of saturated water under atmospheric pressure is presented. Two-phase mixture flow in pool boiling is simulated with the developed two-fluid model and it is coupled with the solving of the transient heat conduction in the heated wall. Nucleate boiling heat transfer coefficient is calculated based on results from the temperature distribution on the heater's surface. The results of these numerical experiments are compared with values calculated with available empirical correlations and with measured values.

In the performed numerical simulations, the dynamics of the bubble generation are modelled through the density of nucleation sites and the bubble residence time on the heater's surface, while the nucleation sites are randomly distributed on the heater`s surface. The numerical results show that the nucleate boiling heat transfer coefficient strongly depends on the characteristics of the wall roughness. Therefore, it is necessary to investigate the surface roughness and to take it into account, in order to obtain the reliable prediction of the nucleate boiling heat transfer coefficient.

Acknowledgments

Nomenclature

a – thermal diffusivity, [m^2s^{-1}]
b – width of the nucleation zone, [m]
C_D – interfacial drag coefficient
C_{sf} – heat transfer coefficient
c_p – specific heat, [$Jkg^{-1}K^{-1}$]
D – diameter, [m]
D_b – bubble departure diameter, [m]
F – force per unit volume, [Nm^{-3}]
g – gravitational acceleration, [ms^{-2}]
h – enthalpy, [Jkg^{-1}]
h_{12} – latent heat of evaporation, [Jkg^{-1}]
Ja – Jacobs number, [–]
k – thermal conductivity, [$Wm^{-1}K^{-1}$]
L_c – water capillary length, [m]
l – characteristic length, [m]
Nu – Nusselt number, [–]
n – density of nucleation sites, [m^{-2}]
Pr – Prandtl number, [–]
p – pressure, [Pa]
$\dot{Q}$ – heat flux, [Ws^{-1}]
q – heat flux, [Wm^{-2}]
q_b – volumetric heat source for bubble generation on the heater's surface, [Wm^{-3}]
q_h – volumetric heat rate, [Wm^{-3}]
T – temperature, [K]
t – time, [s]
u – velocity, [ms^{-1}]

x – co-ordinate, [m]

Greek symbols

α – void fraction
Γ – phase transition rate, [$kgm^{-3}s^{-1}$]
θ – wetting contact angle, [deg]
μ – dynamic viscosity, [Pa·s]
ν – kinematic viscosity, [m^2s^{-1}]
ρ – density, [kgm^{-3}]
σ – surface tension, [Nm^{-1}]
τ – phase change relaxation time, [s]

Subscripts

b – bubble
c – condensation
e – evaporation
fg – fluid gas
k – phase index ($k = 1, 2$)
p – particle
sat – saturation
w – wall
1 – water
2 – steam
21 – interfacial
' – saturated liquid
" – saturated vapor

References

[1] Leidenfrost, J. G., On the Fixation of Water in Diverse Fire (From a Tract about some Qualities of Common Water, 1756), *International Journal of Heat and Mass Transfer, 9* (1966), 11, pp. 1153-1166

[2] Nukiyama, S., Maximum and Minimum Values of Heat Transmitted from Metal to Boiling Water under Atmospheric Pressure (in Japanese), *Journal of the Japanese Society of Mechanical Engineers, 37* (1934), 206, pp. 367-374; *International Journal of Heat and Mass Transfer, 9* (1966), 12, pp. 1419-1433

[3] Kutateladze, S. S., On the Transition to Film Boiling under Natural Convection, *Kotloturbostrenie, 3* (1948), pp. 10-12

[4] Kutateladze, S. S., Hydrodynamic Model of Heat Transfer Crisis in Free-Convection Boiling, *J. Tech. Phys., 20* (1950), 11, pp. 1389-1392

[5] Zuber, N., On the Stability of Boiling Heat Transfer, *ASME J. Heat Transfer, 80* (1958), 2, pp. 711-720

[6] Kutateladze, S. S., Borishanskii, V. M., *A Concise Encyclopedia of Heat Transfer*, Chapter 12, Pergamon Press, New York, USA, 1966

[7] Kutateladze, S. S., *Heat Transfer and Hydrodynamic Resistance: Handbook* (in Russian), Chapter 12.7, Energoatomizdat Publishing House, Moscow, 1990

[8] Kruzhilin, G. N., Free-Convection Transfer of Heat from a Horizontal Plate and Boiling Liquid (in Russian), *Reports of the USSR Academy of Science, 58* (1947), 8, pp. 1657-1660

[9] Mostinski, I. L., Application of the Rule of Corresponding States for Calculation of Heat Transfer and Critical Heat Flux, *Teploenergetika, 4* (1963), p. 66

[10] Rohsenow, W. M., A Method of Correlating Heat Transfer, Data for Surface Boiling of Liquids, *Transactions of the ASME, 74* (1952), Jan., pp. 969-976

[11] Pioro, I. L._, et al._, Nucleate Pool-Boiling Heat Transfer. II: Assessment of Prediction Methods, *International Journal of Heat and Mass Transfer, 47* (2004), 23, pp. 5045-5057.

[12] Dhir, V. K., Mechanistic Prediction of Nucleate Boiling Heat Transfer-Achievable or a Hopeless Task?, *Journal of Heat Transfer*, *128* (2006), Oct., pp. 1-12

[13] Theofanous, T. G._, et al._, The Boiling Crisis Phenomenon Part I: Nucleation and Nucleate Boiling Transfer, *Experimental Thermal and Fluid Science, 26* (2002), 6-7, pp. 775-792

[14] Theofanous, T. G. _et al._, The Boiling Crisis Phenomenon Part II: Dry, out Dynamics and Burnout, *Experimental Thermal and Fluid Science, 26* (2002), 6-7, pp. 793-810

[15] Kim, J., Review of Nucleate Pool Boiling Bubble Heat Transfer Mechanisms, *International Journal of Multiphase Flow, 35* (2009), 12, pp. 1067-1076

[16] Son, G., Dhir, V. K., Numerical Simulation of Nucleate Boiling on a Horizontal Surface at High Heat Fluxes, *International Journal of Heat and Mass Transfer, 51* (2008), 9, pp. 2566-2582

[17] Sanna, C._, et al._, Numerical Investigation of Nucleate Boiling Heat Transfer on Thin Substrates, *International Journal of Heat and Mass Transfer, 76* (2014), Sep., pp. 45-64

[18] Li, Z. D._, et al._, Numerical Simulation of Bubble Dynamics and Heat Transfer with Transient Thermal Response of Solid Wall during Pool Boiling of FC-72, *International Journal of Heat and Mass Transfer, 84* (2015), May, pp. 409-418

[19] Pezo, M., Stevanović, V., Numerical Prediction of Critical Heat Flux in Pool Boiling with the Two-Fluid Model, *International Journal of Heat and Mass Transfer, 54* (2011), 15, pp. 3296-3303

[20] Qi, Y._, et al._, Role of Surface Structure in Heterogeneous Nucleation, *International Journal of Heat and Mass Transfer, 47* (2004), 14, pp. 3097-3107

[21] Fritz, W., Calculate the Maximum Volume of Vapor Bubbles (in German), *Physikalische Zeitschrift, 36* (1935), pp. 379-384

[22] Isachenko, V. P._, et al._, *Heat Transfer*, Mir Publisher, Moscow, 1980, pp. 311-312

[23] Patankar, S. V., *Numerical Heat Transfer and Fluid Flow*, Hemisphere Publishing Corporation, Carlsbad, Cal., USA, 1980